

# The free energy of compressed lattice knots

**EJ Janse van Rensburg**<sup>1</sup>‡

<sup>1</sup>Department of Mathematics and Statistics, York University, Toronto, Ontario  
M3J 1P3, Canada

**Abstract.** The osmotic pressure of a knotted ring polymer in a confining cavity is modelled by a lattice polygon confined in a cube in  $\mathbb{Z}^3$ . These polygons can be knotted and are called lattice knots. In this paper the GAS algorithm [17] is used to estimate the free energy of lattice knots of knot types the unknot, the trefoil knot, and the figure eight knot, as a function of the concentration of monomers in the confining cube. The data show that the free energy is a function of knot type at low concentrations, and (mean-field) Flory-Huggins theory [12, 15] is used to model the free energy as a function of monomer concentration. The Flory interaction parameter of lattice polygons in  $\mathbb{Z}^3$  is also estimated. At critical values of the concentration the osmotic pressure may vanishes, and these critical concentrations, suitably rescaled, is dependent on knot type.

‡ [reensburg@yorku.ca](mailto:reensburg@yorku.ca)

## 1. Introduction

The effects of topology on the free energy of a polymer is a widely studied topic [8, 28, 43]. These effects are important in biological systems [21, 34, 35] since the biological function of DNA and other biopolymers are dependent on the entanglement between polymers and the knotting in polymers [5].

The study of knotting in polymers dates back more than 50 years [9, 10], and continues to be an important factor in the modelling of polymer entropy [8, 28, 44]. It is, for example, known numerically and by rigorous proof, in several random polygon models of ring polymers, that there is a high probability of knotting, at least in the asymptotic regime [20, 33, 37, 41]. The impact of knotting and entanglements on the free energy of a polymer was analysed in a variety of different models [27, 29, 32, 42] and there is now a large literature devoted to knots in models of polymers; see for example references [26, 30, 38, 39, 41].

Knotting in self-avoiding walk models of polymers has received much attention in the literature [18, 31, 41]. The usual model for knotting in ring polymers is a lattice polygon in a three dimensional lattice, often called a *lattice knot*. It is known that the conformational entropy of a lattice knot is a function of its knot type [33, 41]. That is, the conformational entropy of an unknotted cubic lattice polygon is different from that of a polygon of unrestricted knot type [41]; see references [18, 45] for numerical evidence. The entropy of lattice knots continues to be the subject of numerous studies, including more recent work in references [2, 24]. In references [25–27] the effects of a confining space on the entropy of a model of a ring polymer of fixed knot type was examined.

In this paper we look into the entropic properties of a self-avoiding walk model of a confined ring polymer of fixed knot type. The ring polymer is modelled by a closed self-avoiding walk (called a *lattice polygon*) confined to a cube in the cubic lattice  $\mathbb{Z}^3$  (see figure 1 for the two dimensional analog of this model). A polygon confined to a cube will be called a *compressed polygon*, and if its knot type is fixed, then it is a *compressed lattice knot*.

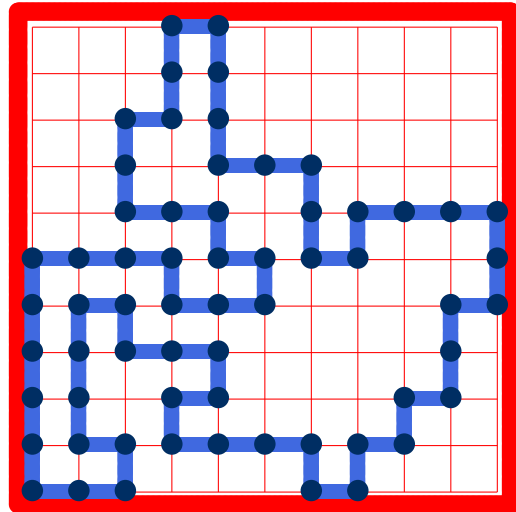


Figure 1: A lattice polygon confined to a square in  $\mathbb{Z}^2$  is the a dimensional model of a ring polymer and compressed in a cavity. In this particular diagram the length of the side of the confining square is 10, and it contains  $11^2 = 121$  sites. We say that the *dimension* of the confining square is 11 and its *volume* is 121.

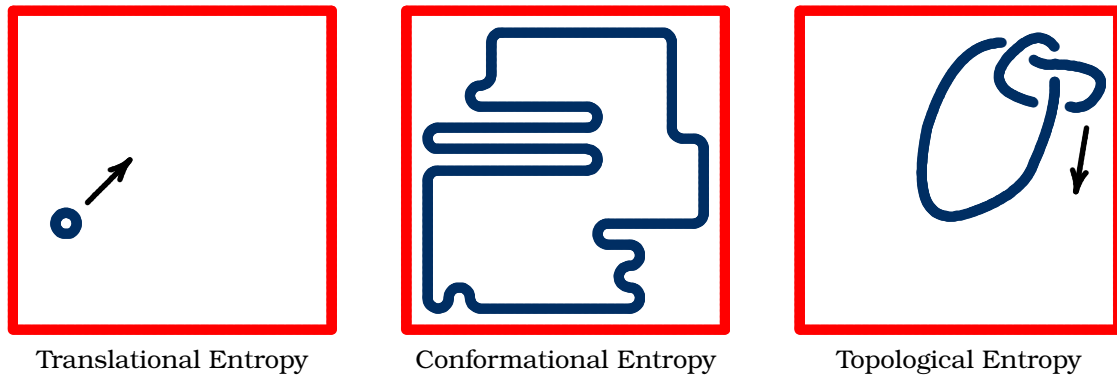


Figure 2: The entropy of a confined ring polymer of length  $n$  in a square or cube of dimension  $L^d$ . If the polymer is very short then it gains entropy from translational degrees of freedom. If it is long, then its entropy is primarily determined by conformational degrees of freedom. The crossover between the translational and conformational regimes should occur when the linear extent of the polymer approaches  $L$ . Since the linear extent of an unconfined polygon is  $O(n^\nu)$ , this crossover occurs when  $O(n^\nu) \sim L$ , where  $\nu$  is the metric exponent of the polymer. In a good solvent the Flory values of  $\nu$  are  $\nu = \frac{3}{4}$  if  $d = 2$ , and  $\nu = \frac{3}{5}$  if  $d = 3$ . The concentration of monomers at the crossover is  $O(n/V) = O(L^{1/\nu-d})$  since the dimension of the confining cube is  $V = L^d$ . That is, in  $d = 2$  the crossover concentration is  $\phi_a = O(L^{-2/3})$ , and, in  $d = 3$ ,  $\phi_a = O(L^{-4/3})$ . That is, with increasing  $L$  the crossover occurs at decreasing concentration. If  $d = 3$  then the polygon may be knotted, and there are topological degrees of freedom contributing to the free energy (right panel).

Such compressed lattice polygons are models of biopolymers in confined spaces (such as in living cells) [7, 9]. Other models of compressed polygons were considered in references [22, 23], as a coarse grained lattice model, and using a bond fluctuation model in reference [4].

We are particularly interested in the following questions: (1) How are the translational and configurational free energy of the polygon dependent on the concentration of monomers (modelled by vertices in the polygon) in the confining cube, and (2) what is the impact of topology (that is, of knot type) on the free energy of the polymer?

With respect to the first question, the model is a lattice polygon confined to a cube in  $\mathbb{Z}^3$  (see reference [14] for a model of a self-avoiding walk confined to a square in the square lattice). The confining cube has side-length  $L-1$  and contains  $L^3$  lattice sites – in this case the *dimension* of the cube is said to be  $L$  and its *volume* is  $V = L^3$ . The concentration  $\phi$  of the lattice polygon is the number of vertices per unit volume.

There are both translational and conformational contributions to the entropy in the model, as shown in figure 2. At low concentrations the polygon is very short, and it has low conformational entropy but can be translated inside the (relatively large) confining space (see the left panel in figure 2). That is, there are translation degrees of freedom which makes the dominant

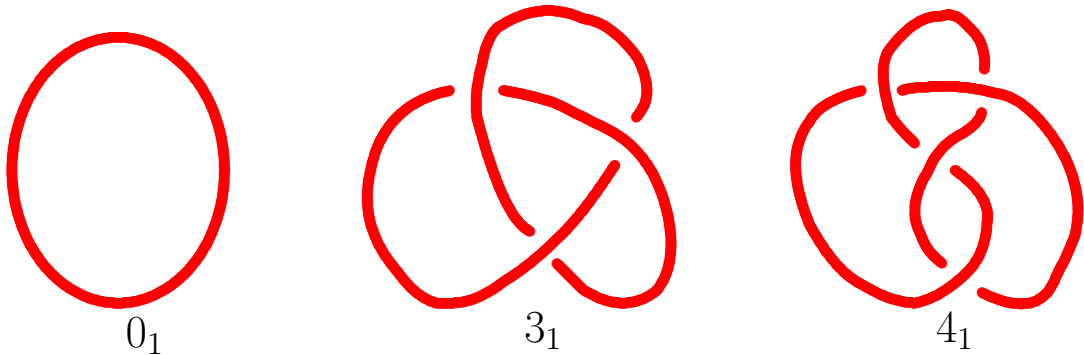


Figure 3: The unknot ( $0_1$ ), the trefoil ( $3_1$ ) and the figure eight ( $4_1$ ).

contribution to the entropy. For a polygon of length  $n$  in a cube of dimensions  $L$  this is the low concentration regime, and it is encountered when  $n \ll L$ .

At high concentrations, on the other hand, the polygon has no translational degrees of freedom, but a large number of conformations; see the middle panel of figure 2. In this case the dominant contributions to the entropy are due to conformational degrees of freedom. The entropy makes a contribution to the free energy of the model. Thermodynamic quantities (for example, the osmotic pressure) can be determined from the free energy, and these are functions of the concentration  $\phi$ . The functional dependence of the free energy on  $\phi$  can be described using Flory-Huggins theory [7, 12, 13, 15].

In this paper we proceed by numerically estimating the free energy in a model of compressed lattice knots, and then investigating the dependence of the free energy and the osmotic pressure on the concentration of monomers and on the knot type of the lattice knot, for the knot types the *unknot*  $0_1$ , the *trefoil knot*  $3_1$ , and the *figure eight knot*  $4_1$ ; see figure 3.

The compressed lattice knot will have a free energy dependent on knot type, and this dependence will be due, in some part, to the topological differences between knot types. We will present data that show, in particular, for lattice polygons at low concentration, that there is a substantial dependence on knot type.

In section 2 a short review of Flory-Huggins theory is given, with the emphasis of making a connection between the free energy per unit volume of a compressed lattice polygons, and the *free energy of mixing* in Flory-Huggins theory (the free energy of mixing is obtained by including energy terms due to monomer-solvent interactions, and discarding all terms which are constant, or linear in the concentration, from the free energy).

I present numerical data on this model in section 3. By Flory-Huggins theory to model the free energy of compressed lattice knots, the Flory interaction parameter  $\chi$  for confined lattice knots is estimated:

$$\chi = 0.18 \pm 0.03. \quad (1)$$

The osmotic pressure is also determined using a numerical derivative of the free energy.

It is also found that the osmotic pressure, for the knot types  $0_1$ ,  $3_1$  and  $4_1$ , is negative for low concentrations. For the unknot  $0_1$  the osmotic pressure goes through a minimum at a critical concentration  $\phi_c \simeq 0.209 L^{-4/3}$  where the dimensions of the confining cube is  $L^3$ . The osmotic pressure also vanishes at the concentrations  $\phi_0 \simeq 0.149 L^{-4/3}$  and  $\phi_m \simeq 0.286 L^{-4/3}$ . In the interval  $(\phi_0, \phi_m)$  the osmotic pressure is negative, and and otherwise it is positive.

For the knot types  $3_1$  and  $4_1$  a different result is obtained. The osmotic pressure vanishes at just one concentration; namely at  $\phi_0 \simeq 3.94 L^{-4/3}$  for  $3_1$  and  $\phi_0 \simeq 4.48 L^{-4/3}$  for the knot type  $4_1$ . For low concentrations  $\phi < \phi_0$ , the osmotic pressure for these knot types remains negative, in contrast of the case for the unknot, where the osmotic pressure becomes positive if the concentration drops low enough. For  $\phi > \phi_0$  the osmotic pressure for the knot types  $3_1$  and  $4_1$  is positive and increasing.

In section 4 the paper is concluded with a few final remarks.

## 2. Flory-Huggins theory and the free energy of compressed lattice knots

Flory-Huggins theory [13, 15] is a mean field theory for modelling the free energy of concentrated solutions of polymers or of polymer melts. The theory is based on (1) a mean field estimate of the entropy, and (2) a second order approximation of monomer-monomer and monomer-solvent interactions. The theory is concerned with the *free energy of mixing*, rather than the total free energy, and so ignores linear terms contributing to the total free energy.

If a single chain is considered, then the entropy per unit volume  $V$ , of a polymer in a confining space, is estimated by

$$-S_{site}(\phi) = \frac{\phi}{n} \log \frac{\phi}{n} + (1 - \phi) \log(1 - \phi) \quad (2)$$

where  $\phi = \frac{n}{V}$  is the volume fraction (or concentration) of monomers in a chain of length  $n$  (degree of polymerization) [15].

The entropy of mixing [12] is the difference between  $S_{site}(\phi)$  and the weighted average of the entropy of pure solvent  $S_{site}(0)$ , and pure polymer  $S_{site}(1)$ :

$$-S_{mix} = -S_{site}(\phi) + (1 - \phi)S_{site}(0) + \phi S_{site}(1) = \frac{\phi}{n} \log \phi + (1 - \phi) \log(1 - \phi). \quad (3)$$

This cancels terms linear in  $\phi$ .

The energy of mixing per site has contributions for solvent-solvent, monomer-monomer and monomer-solvent interactions. For example, the contribution of monomer-solvent interactions is approximated by  $E_{MS} = T \chi_{MS} \phi (1 - \phi)$ , and is a *two-body* approximation, leaving out higher order

contributions. Contributions from monomer-monomer and solvent-solvent interactions are similarly given by  $E_{SS} = T \chi_{SS} (1-\phi)^2$  and  $E_{MM} = T \chi_{MM} \phi^2$ . Collecting the second order contributions, and then computing the energy of mixing similar to  $S_{mix}$  above, give the energy of mixing

$$E_{mix} = T \chi \phi (1 - \phi). \quad (4)$$

where  $\chi = \chi_{MS} - \frac{1}{2}(\chi_{MM} + \chi_{SS})$ .

The *mean field free energy of mixing per site*  $F_{mix}$  is given by adding to  $-S_{mix}$  the energy of mixing  $\frac{1}{T}E_{mix}$  per site [7]:

$$\frac{1}{T} F_{mix} = \frac{1}{T} E_{mix} - S_{mix} = \frac{\phi}{n} \log \phi + (1 - \phi) \log(1 - \phi) + \chi \phi (1 - \phi), \quad (5)$$

Expanding for small values of  $\phi$  gives

$$\frac{1}{T} F_{mix} = \frac{\phi}{n} \log \phi + \frac{1}{2}(1 - 2\chi) \phi^2 + \frac{1}{6}\phi^3 + \dots \quad (6)$$

The (Edwards) *excluded volume parameter* is the coefficient of the quadratic term given by  $v = 1 - 2\chi$  [11]. If  $v = 0$  then the polymer is in  $\theta$ -conditions and the first correction to  $\frac{\phi}{n} \log \phi$  in  $F_{mix}$  is the third order term in  $\phi$ . If  $v < 0$  then the polymer is in a poor solvent, and if  $v > 0$  it is in a good solvent. Notice that there are no linear terms in  $\phi$  in the expansion and that these linear contributions are deliberately left away in Flory-Huggins theory.

The parameter  $\chi$  is the *Flory interaction parameter*, and it is a measure of the (repulsive) interactions between solvent molecules and monomers.  $\chi$  tends to be positive [7] and increasing with  $T$ . Good solvents have small values of  $\chi$  and if  $\chi = 0$  then the solution is said to be “athermal”. When  $\chi = \frac{1}{2}$  then the solvent is said to be marginal and the polymer is in  $\theta$ -conditions. For  $\chi > \frac{1}{2}$  the solvent is poor and the polymer may collapse from a coil to a globule phase [6, 40].

The derivation of  $F_{mix}$  discards terms linear in  $\phi$ , and also does not include multi-body interactions between monomers and solvent molecules. Instead, it only includes a two-body interaction between monomers and solvent molecules, and introduces the term  $\chi \phi (1 - \phi)$  to account for this. The parameter  $\chi$  is the Flory interaction parameter. If  $\chi < 0.5$  the polymer is in a good solvent, if  $\chi > 0.5$  the solvent is poor. The case  $\chi = 0$  is called “athermal”, and if  $\chi = 0.5$  then the series expansion of  $F_{mix}$  has no second order terms due to cancellations, and the polymer is in  $\theta$ -conditions [7].

The free energy of the model in figure 1 is given by  $F_{tot} = \log p_{n,L}$ , where  $p_{n,L}$  is the total number of conformations of the lattice polygon with placements in the containing volume  $V$  of dimensions  $L^3$  counted as different. The free energy per unit volume (or per lattice site) is given by

$$F_V = -\frac{1}{V} \log p_{n,L}. \quad (7)$$

The Flory free energy of mixing  $F_{mix}$  in equation (2) is also a free energy per unit volume, and so is related to  $F_V$ . Since linear terms were discarded in

the mean field derivation of  $F_{mix}$ , the free energy of mixing  $F_{mix}$  is a mean approximation to  $F_V$  up to missing linear terms in  $\phi$  (and also up to cubic and higher order terms in  $\phi$ ). That is, a mean field assumption for  $F_V$ , based on the Flory-Huggins free energy of mixing, would be

$$F_V = a_0 \phi + \frac{\phi}{n} \log \phi + (1 - \phi) \log(1 - \phi) - \chi \phi^2, \quad (8)$$

where  $a_0$  is a constant.

The osmotic pressure is defined in terms of  $F_V$  by  $\Pi = -\frac{d}{dV} F_{tot} = \phi^2 \frac{\partial}{\partial \phi} \left( \frac{1}{\phi} F_V \right)$  (see equation III.12 in reference [7]), and, since the linear term in equation (8) vanishes when the derivative is taken, this gives the following Flory-Huggins mean field expression for  $\Pi$ :

$$\Pi = \phi^2 \frac{\partial}{\partial \phi} \left( \frac{1}{\phi} F_V \right) = \phi^2 \frac{\partial}{\partial \phi} \left( \frac{1}{\phi} F_{mix} \right) = \frac{1}{V} - \log(1 - \phi) - \phi - \chi \phi^2, \quad (9)$$

where it was noted that  $\phi = \frac{n}{V}$ .

The term  $\frac{1}{V}$  in equation (9) quickly vanishes when  $V$  increases, and so, even for small values of  $L$ , it will be left away in some cases. This expression should break down for high concentrations, since  $\Pi$  is a derivative of  $F_V$  and the Flory-Huggins approximation has a logarithmic singularity when  $\phi \rightarrow 1^-$ .

In figure 4 a schematic diagram for  $F_V$  with  $\chi = \frac{1}{4}$  and  $a_0 = -0.10$  is shown.  $F_V$  is represented by the solid curve and it is a convex function of  $n$ . The osmotic pressure  $\Pi$  is the dashed curve, and is generally positive and increasing with concentration  $\phi$ .

The free energy per monomer of the lattice knot is given by

$$f_t(\phi) = -\frac{1}{n} \log p_{n,L}(K) = \frac{1}{\phi} F_V. \quad (10)$$

Using the model in equation (18), the mean field Flory-Huggins expression for  $f_t(\phi)$  is

$$f_t(\phi) = a_0 + \frac{1}{V\phi} \log \phi + \frac{1-\phi}{\phi} \log(1 - \phi) - \chi_L \phi, \quad (11)$$

where the possibility that  $\chi_L$  is a function of  $L$  is explicitly indicated. Taking  $L \rightarrow \infty$  (and so  $V \rightarrow \infty$ ) gives the limiting curve

$$\lim_{L \rightarrow \infty} f_t(\phi) = a_0 + \frac{1-\phi}{\phi} \log(1 - \phi) - \chi_{saw} \phi, \quad (12)$$

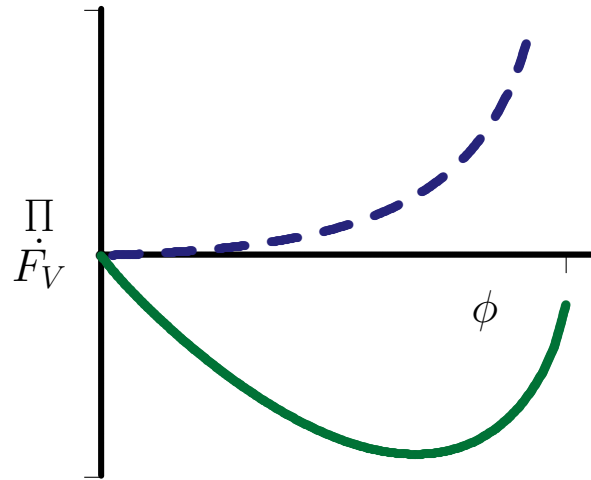


Figure 4: The Flory-Huggins total free energy per lattice site  $F_V$  (solid curve) and the osmotic pressure (dashed curve) which are obtained from the free energy of mixing  $F_{mix}$  modified by subtracting from it the linear term  $0.10 \phi$ . In this schematic drawing,  $N = 10$  and  $\chi = \frac{1}{4}$ .

provided that  $\phi > 0$  and where  $\chi_{\text{saw}}$  is the limiting value of the Flory interaction parameter. The limit  $\phi \rightarrow 0^+$  of the right hand side gives

$$\lim_{\phi \rightarrow 0^+} \lim_{L \rightarrow \infty} f_t(\phi) = a_0 - 1. \quad (13)$$

This is the zero concentration limit, and this should be equal to  $-\log \mu_3(K)$ , where  $\mu_3(K)$  is the growth constant of lattice polygons of knot type  $K$ . To see this, place a polygon of length  $L$  and knot type  $K$  in a cube of dimensions  $L^3$ . The number of polygons in the cube is  $O(L^3) \times p_L(K)$  (where  $p_L$  is the number of polygons of length  $L$  and knot type  $K$ ). Taking logarithms, dividing by  $L$  and letting  $L \rightarrow \infty$  gives  $-\log \mu_3(K)$  while the concentration goes to zero as  $O(L^{-2})$ . This shows that  $a_0 = 1 - \log \mu_3(K)$ . That is, fitting numerical data against  $f_t(\phi)$  for finite values of  $V$  should give estimates of  $a_0$  which approaches  $1 - \log \mu_3(K)$  as  $V$  increases, while  $\chi_L$  approaches a limiting value which is equal to the Flory interaction parameter of the polygons.

### 3. Numerical data

The GAS algorithm [16, 17] was implemented with BFACF elementary moves [1, 3, 19] to sample lattice knots in  $\mathbb{Z}^3$  along a Markov Chain in state space [17]. Confining the lattice knot to a cube reduces the size of state space, and creates lattice knot irreducibility classes fitting inside the cube. This reduction in the size of the irreducibility class is a model of the reduction in entropy when a ring polymer is confined to a cavity. In each model (defined by the knot type of the compressed lattice knots, and by the dimension of the confining cube) there is a irreducibility class which contains the minimum length lattice knots.

In the case of the unknot there are three minimal length realisations of length 4 in the cubic lattice, namely the unit square in each of the three lattice planes in  $\mathbb{Z}^3$ . When confined in a cube of dimension  $L$  (and side length  $L-1$ ) these minimal length unknotted polygons are members of an irreducibility class which will be called the *natural class* of compressed (unknotted) polygons. The number of states of minimal length in the natural class of unknotted lattice knots can be counted, and these numbers are shown in the second column of table 1; for a cube of dimension  $L$  the number of minimal length lattice knots of length 4 is  $3L(L-1)^2$ . For example, if  $L = 2$  (the cube with 8 sites), there are 6 polygons of length 4.

The situation is more complicated if the polygons are knotted. For example, for lattice knots of knot type trefoil, in a cube of dimension 5 (with  $5^3$  sites) a computer count gives 30104 lattice knots of minimal length  $n = 24$  which will fit inside the cube (with lattice knots equivalent under translations counted as distinct). These minimal length lattice knots are members of the

natural class of compressed lattice knots of knot type  $3_1$  (the trefoil) in the cube of dimension 5 and 125 lattice sites.

More generally, for the knot type  $3_1$  there are 3328 distinct (up to translation) realisations of minimal length lattice knots of length ( $n = 24$ ) [36]. In a cube of dimension 3 (with  $3^3 = 27$  sites), none of these minimal lattice knots will fit, and so the natural class is empty. In a cube of dimension 4 (with  $4^3 = 64$  sites) there are 3304 minimal length lattice knots which can be placed. This gives a natural class of (with lattice knots equivalent under translations counted as distinct). There are also 24 minimal length lattice knots of type  $3_1$  which will not fit into the cube of dimensions 4. In other words, the natural class of minimal length lattice knots does not include representatives of these polygons, and this is indicated by the \* in table 1. The GAS algorithm finds all these 4168 states (that is, if rigid rotations and reflections of the entire polygon is added to the BFACF moves, then all minimal length states inside a cube of dimension 4 is found by the algorithm).

$L^3$	$0_1$ ( $n = 4$ )	$3_1$ ( $n = 24$ )	$4_1$ ( $n = 30$ )
$2^3$	6	—	—
$3^3$	36	—	—
$4^3$	108	4168*	864*
$5^3$	240	30104	18048
$6^3$	450	97752	73440
$7^3$	756	227080	188928
$8^3$	1176	438056	386400
$9^3$	1728	750648	687744
$10^3$	2430	1184824	1114848
$11^3$	3300	1760552	1689600
$12^3$	4356	2497800	2433888
$13^3$	5616	3416536	3369600
$14^3$	7098	4536728	4518624
$15^3$	8820	5878344	5902848

Table 1: Counts of minimal length polygons in  $L^3$

of type  $4_1$  (the minimal length is 30) [36]. None of these minimal length lattice knots can be placed in a cube of dimension 3, but a total of 864 lattice knots of length 30 and type  $4_1$  can be placed in a cube of dimension 4. The GAS algorithm, implemented with rigid rotations and reflections, detects all 864 minimal length states in a cube of dimension 4, and so the natural class for lattice knots of type  $4_1$  in a cube of dimension 4 is defined in this way. If the cube has dimension 5, then the algorithm detects all 3648 minimal length

All minimal length lattice knots of type  $3_1$  can be placed inside a cube of dimension  $5^3$ , and the natural class contains 30104 minimal length lattice knots. The algorithm, if implemented with rigid rotations and reflections of the confined lattice knot inside the cube, finds all these states, so that the natural class contains all minimal length lattice knots in a cube of dimensions  $5^3$ . This is similarly true for larger cubes- the number of minimal length states in each case is listed in table 1.

Similarly, there are 3648 minimal length lattice knots

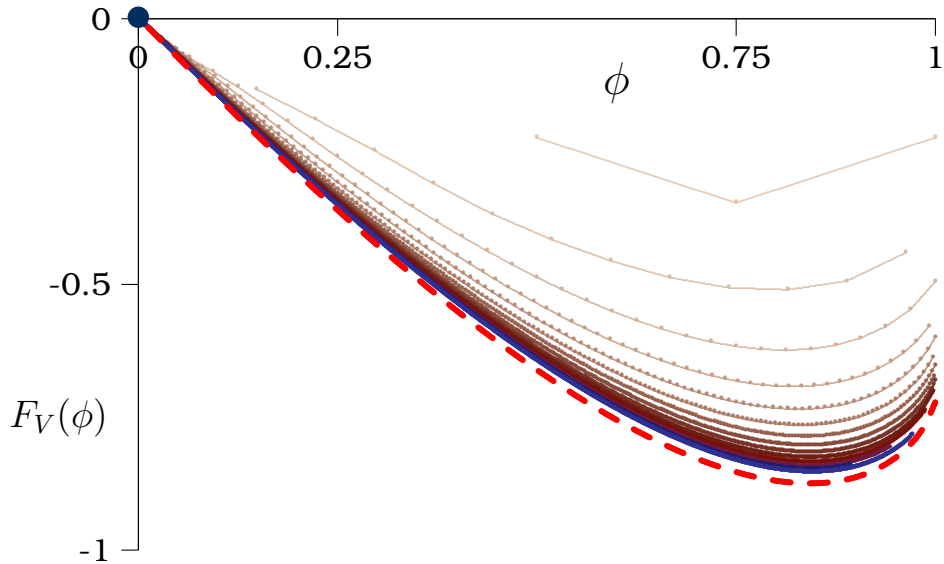


Figure 5: The free energies  $F_V(\phi)$  of compressed unknotted lattice knots confined to cubes of dimensions  $L$ , with  $L \in \{3, 4, 5, \dots, 12\}$ . With increasing values of  $L$  the curves systematically decrease to an apparent limiting curve. The dashed line is the limiting curve given by Flory-Huggins theory (see equation (18)).

lattice knots of type  $4_1$ , and they can be placed 18048 distinct ways, as shown in table 1.

These observations are similarly true for larger cubes and the number of states of minimal length in the natural class is listed in table 1 and are detected by the algorithm.

The GAS algorithm was implemented using the data in table 1 and it sampled along GAS sequences in parallel on a multiprocessor computer. A total of 400 sequences were realised, each of length  $2L \times 10^6$  iterations. For example, for  $L = 10$ , a total of  $2 \times 10^7$  lattice knots in a cube of dimension 10 were sampled along each sequence, for a total of  $8 \times 10^9$  iterations in total. The resulting data are approximate counts of lattice knots of length  $n$  in the natural class in a cube of dimension  $L$ ; these are estimates of  $p_{n,L}(K)$ , the number of lattice knots in the natural class, of knot type  $K$ , and length  $n$ .

In figure 5 the estimates of the free energy per lattice site in cubes of volume  $V = L^d$ ,  $F_V(\phi) = \frac{1}{V} \log p_{n,L}$ , are plotted as a function of the concentration of vertices  $\phi = \frac{n}{V}$  for unknotted lattice polygons. The general appearance of these curves is similar to the curve due to Flory-Huggins theory shown in figure 1.

### 3.1. Unknotted compressed lattice knots

**3.1.1. The free energy of compressed unknotted lattice knots:** The Flory-Huggins mean field expression for  $F_V(\phi)$  is given by equation (8). Since  $\phi = \frac{n}{V}$ , the contribution of the second term to this expression is small for larger

values of  $\phi$ , and the approximation

$$F_V(\phi) \simeq a_0\phi + (1 - \phi)\log(1 - \phi) - \chi_{01}\phi^2 \quad (14)$$

may be used to model the data in figure 5. For example, when  $L = 10$  then a least squares fit to the data gives

$$F_V(\phi)|_{L=10} \approx -0.4252\phi + (1 - \phi)\log(1 - \phi) - 0.2388\phi^2. \quad (15)$$

This suggests that  $a_0 = -0.4252\dots$ , and the estimate for  $\chi_{01}$  is a finite  $L$  value of the Flory-Huggins interaction parameter:  $\chi_{01}|_{L=10} = 0.2388\dots$

$L$	$\chi_{01}$	$\chi_{31}$	$\chi_{41}$
3	0.4372	—	—
4	0.3611	0.9796	1.2820
5	0.3084	0.5983	0.7395
6	0.2810	0.4185	0.4913
7	0.2617	0.3333	0.3737
8	0.2514	0.2905	0.3189
9	0.2437	0.2662	0.2814
10	0.2388	0.2524	0.2619
11	0.2335	0.2433	0.2501
12	0.2284	0.2367	0.2396
13	0.2188	0.2235	0.2272
14	0.2122	0.2165	0.2203
15	0.2176	0.2246	0.2239

Table 2: Estimated Flory interaction parameters from  $F_V(\phi)$ .

approach a limiting free energy. There is a concentration  $\phi^*$  where  $f_t(\phi)$  has a local minimum.

When  $\phi < \phi^*$  the lattice knot is short and translational degrees of freedom may make a contribution to the free energy. As  $L$  increases  $\phi^*$  should decrease to zero, and the local minimum in the free energy to  $-\log \mu_3(\emptyset)$ , where  $\mu_3(\emptyset)$  is the growth constant of unknotted lattice polygons (see, for example, reference [18, 45]). This is seen by noticing that at a concentration  $\phi_L = \frac{L}{V}$  polygons have length  $L$  and the total number of states is of order  $O(L^3 p_{L,L}) \simeq O(L^3 p_L(\emptyset))$ , where  $p_L(\emptyset)$  is the number of unknotted lattice polygons of length  $L$ . Taking logarithms, dividing by  $L$ , and taking  $L \rightarrow \infty$  gives  $\log \mu_3(\emptyset)$ , and  $\phi_L \rightarrow 0^+$ .

The Flory-Huggins approximation to  $f_t(\phi)$  is given by equation (12):

$$f_t(\phi) \simeq a_0 + \frac{1-\phi}{\phi} \log(1 - \phi) - \chi_{01}\phi. \quad (16)$$

The remaining estimates of  $\chi_{01}$  for  $3 \leq L \leq 15$  are listed in the second column of table 2. These data are plotted in figure 6 against  $\frac{1}{n}$ . There remains some curvature in the data for small values of  $L$ , but an extrapolation by a quadratic polynomial for  $L \geq 7$  gives the limiting value  $\chi_{01} = 0.18$ , while a linear extrapolation also gives  $\chi_{01} = 0.18$ . Including all the data instead gives  $\chi_{01} = 0.18$  (a quadratic extrapolation), and  $\chi_{01} = 0.15$  (a linear extrapolation). Thus, we take as our best estimate  $\chi_{01} = 0.18(3)$ .

The free energy per monomer  $f_t(\phi)$  (see equation (10)) is plotted figure 7. The sharp decrease in  $f_t(\phi)$  at low concentration is due to the contribution of translational degrees of freedom to the entropy when the lattice polygon is very short, and can explore the volume of the confining cube freely. With increasing values of  $L$   $f_t(\phi)$  appears to

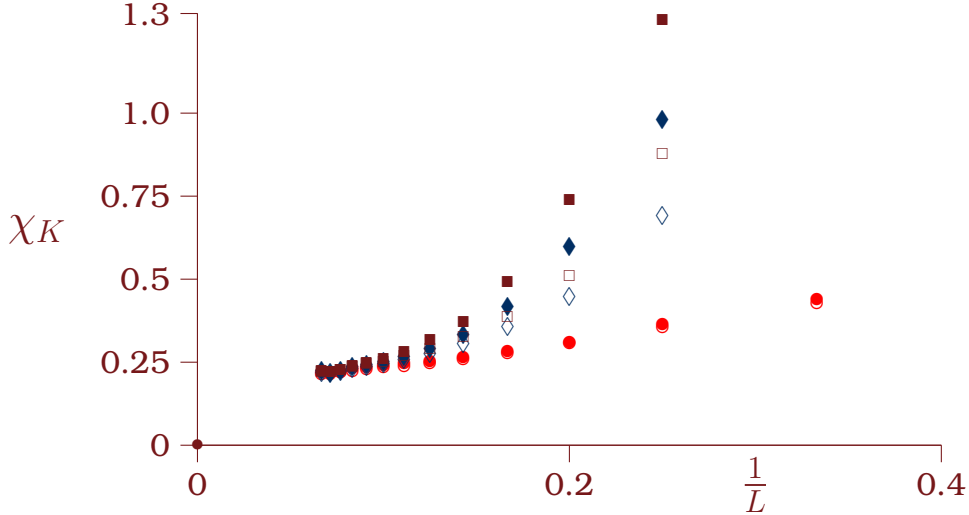


Figure 6: Estimates of the Flory Interaction parameter  $\chi_K$  for knot types the unknot (●), the trefoil (♦), and the figure eight knot (■). The solid points are estimates determined from the free energy  $F_V$ , while open points are estimates determined from  $f_t$ . The data are plotted against  $1/L$  and clearly approaches a limiting value as  $L$  increases.

Taking the derivative of the right hand side shows that this is an increasing function of  $\phi$ . However the curves in figure 7 are not monotone, but go through a local minimum at a critical concentration  $\phi^*$  before increasing monotone as  $\phi$  approaches 1.

In order to estimate the Flory Interaction Parameter  $\chi_{10}$  from these data, a least squares fit of equation (16) was done against the data for  $\phi > \phi^*$  (that is, on numerical data for concentrations where  $f_t(\phi)$  is monotone increasing). This is shown in figure 8: The location of the local minimum in  $f_t(\phi)$  is indicated by a bullet. It is expected that  $\phi^* \rightarrow 0^+$  as  $L \rightarrow \infty$ . In this case  $f_t(\phi^*) \rightarrow -\log \mu_3(\emptyset)$  if  $L \rightarrow \infty$ , this shows that  $a_0 \rightarrow 1 - \log \mu_3(\emptyset)$  as  $L \rightarrow \infty$  in equation (16). The bullet on the vertical axes in figures 7 and 8 denotes  $-\log \mu_3(\emptyset)$ .

The least squares estimates of  $\chi_{10}$  from the data in figure 7 are functions of  $L$ . As  $L$  increases these should give an extrapolated estimate of the Flory Interaction Parameter  $\chi_{10}$  of unknotted lattice polygons. In a cube of dimensions  $9^3$  (as in figure 8), a least squares fit gives  $a_0|_{L=9} = -0.4107\dots$  and

$L$	$\chi_{01}$	$\chi_{31}$	$\chi_{41}$
3	0.4265	—	—
4	0.3530	0.6906	0.8784
5	0.3046	0.4482	0.5115
6	0.2748	0.3564	0.3886
7	0.2561	0.3053	0.3265
8	0.2437	0.2760	0.2895
9	0.2370	0.2569	0.2686
10	0.2320	0.2471	0.2531
11	0.2260	0.2383	0.2450
12	0.2220	0.2325	0.2370
13	0.2165	0.2231	0.2270
14	0.2192	0.2180	0.2225
15	0.2132	0.2193	0.2218

Table 3: Estimated Flory interaction parameters from  $f_t$

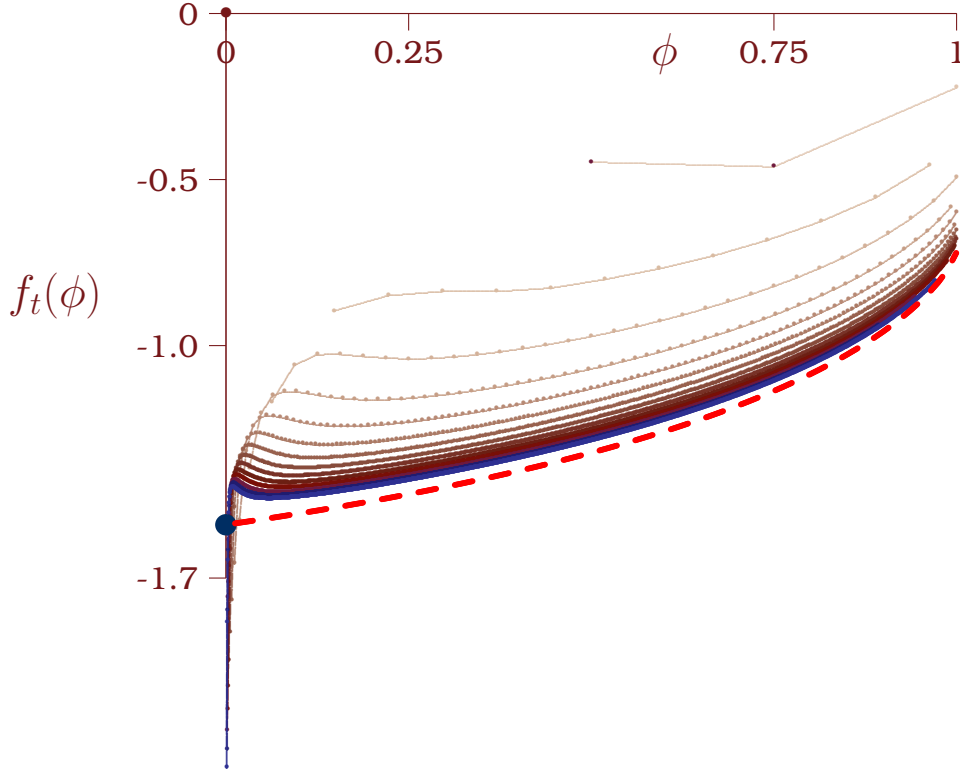


Figure 7: The free energies  $f_t(\phi)$  of compressed unknotted lattice polygons confined in cubes of dimensions  $L^3$ , with  $L \in \{3, 4, 5, \dots, 15\}$ . With increasing values of  $L$  the curves systematically decrease to an apparent limiting curve. Notice the behaviour at small  $\phi$  where there is a sharp decrease in  $f_t(\phi)$  due to translational degrees of freedom at low concentrations. The dashed line is the limiting curve given by the approximation in equation (16) with  $a_0 = 1 - \log \mu_3(\emptyset)$  and  $\chi_{01} = 0.18$ .

$\chi_{01}|_{L=9} = 0.2370\dots$ . The estimates of  $\chi_{01}$  for the values of  $L \in \{3, 4, 5, \dots, 15\}$  are listed in table 3.

Extrapolating the data with a quadratic gives the limiting estimate  $\chi_{01} = 0.17$ , and a linear extrapolation of the data for  $L \geq 9$  gives  $\chi_{01} = 0.18$ . These results are consistent with those determined from  $F_V$  above.

Taken together, the consistent results for the Flory interaction parameter determined from  $F_V(\emptyset)$  and  $f_t(\emptyset)$  indicates the best numerical estimate for  $\chi_{01}$  from the numerical data in this study:

$$\chi_{01} = 0.18 \pm 0.03. \quad (17)$$

The value of  $a_0$  in equation (14) is given by  $1 - \log \mu_3(\emptyset)$ , and since numerical results indicate that  $\mu_3(\emptyset) \approx \mu_3$  to at least 5 significant digits [18], one may approximate  $a_0 \approx 1 - \log \mu_3 = -0.5442\dots$ . This gives the model

$$F_V(\emptyset) \approx -0.544\phi + (1 - \phi) \log(1 - \phi) - 0.18\phi^2. \quad (18)$$

This is plotted as the dashed curve in figure 5 and it is a good approximation of  $F_V(\emptyset)$  over the entire range of  $\phi \in [0, 1]$ . Since  $f_t(\emptyset) = \frac{1}{\phi}F_V(\emptyset)$ , the model

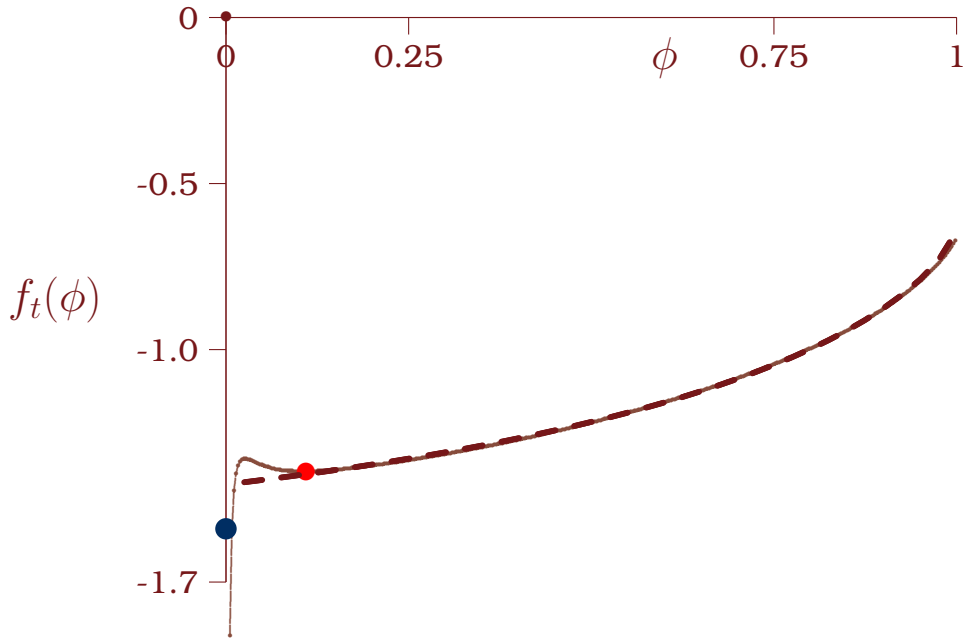


Figure 8: The free energies  $f_t(\phi)$  of compressed unknotted lattice polygons in a cube of dimensions  $9^3$ . The local minimum is indicated by the bullet and it occurs at a concentration  $\phi^*$ . If  $L \rightarrow \infty$ , then  $\phi^*$  should approach zero, and the local minimum in the free energy should approach  $-\log \mu_3(\emptyset)$ , where  $\mu_3(\emptyset)$  is the growth constant of lattice polygons of knot type  $\emptyset$ . In this case  $L = 9$ , the local minimum is at  $-1.3697$ , and the critical concentration is  $\phi^* = 0.1097$ . The dashed curve is the least squares fit of equation (16) for  $\phi > \phi^*$ .

above is also a model for the free energy per unit length, and this is shown by the dashed curve in figure 7.

**3.1.2. The osmotic pressure of compressed unknotted lattice knots:** The osmotic pressure  $\Pi_\emptyset$  of unknotted compressed lattice knots can be calculated from equation (9) and the data for the free energy per site  $f_t(\phi)$ .  $\Pi_\emptyset$  is related to the derivate of  $f_t(\phi)$ , and the data were smooth enough to make it possible to find numerical estimates of the osmotic pressure by using a numerical derivative of  $F_V$  to  $\phi$ . In particular, noting that if  $V$  is fixed and  $\phi = \frac{n}{V}$ , a central second order numerical approximation to the derivative was used:

$$\frac{\partial}{\partial \phi} f_t(\phi) \approx D_\phi f_t(\phi) = \frac{V}{12} \left( -f_t\left(\frac{n+2}{V}\right) + 8f_t\left(\frac{n+1}{V}\right) - 8f_t\left(\frac{n-1}{V}\right) + f_t\left(\frac{n-2}{V}\right) \right). \quad (19)$$

The approximation to the osmotic pressure is

$$\Pi_\emptyset \approx \frac{n^2}{V^2} D_\phi f_t(\phi), \quad (20)$$

at the concentration which is given by the midpoint value  $\phi = \frac{n}{V}$  above.

$\Pi_\emptyset(\phi)$  is plotted against  $\phi$  in figure 9. There is a very good data collapse to a single curve for  $\Pi_\emptyset$ , and the osmotic pressure generally increases with  $\phi$  as expected. The numerical derivative is very sensitive to noise in the data, and the scattering of the points are due to inaccuracies in the numerical data.

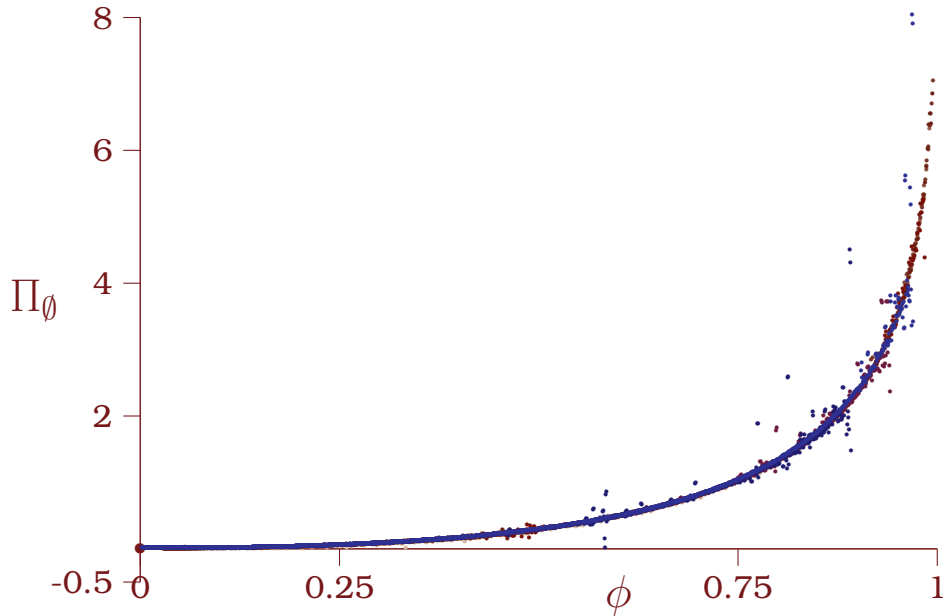


Figure 9: Osmotic pressure  $\Pi_\emptyset$  for compressed unknotted lattice polygons determined by equation (19).

Putting  $\chi = 0.18$  in equation (9) gives an expression for the osmotic pressure plotted in figure 9. This expression is a good approximation for  $\Pi_\emptyset$  for  $\phi < \frac{1}{2}$ , but it deviates significantly from the data for high concentrations – this is not unexpected, since the osmotic pressure is a derivative quantity, and the approximation using the Flory-Huggins expression for the free energy ignored higher order terms which are likely becoming important for higher values of  $\phi$ .

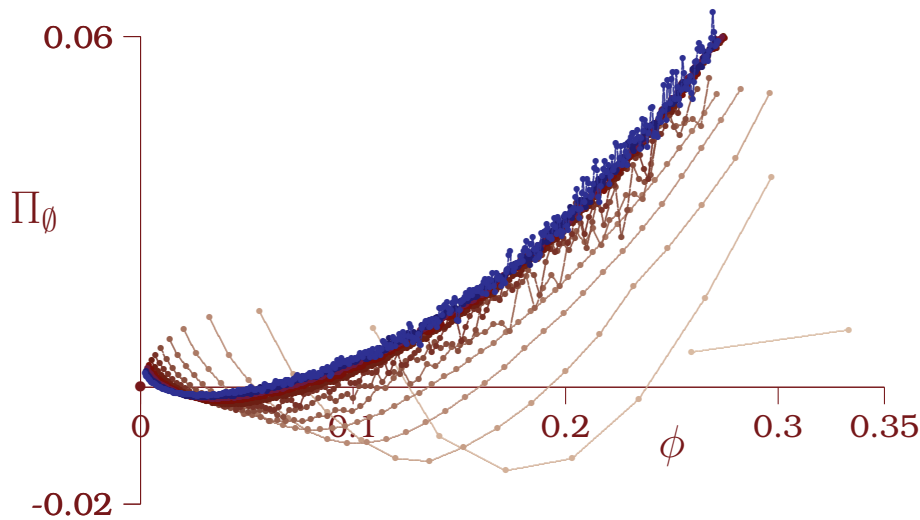


Figure 10: The osmotic pressure  $\Pi_\emptyset$  for compressed unknotted lattice polygons at low concentration. The pressure turns negative for low values of the concentration, and has a minimum at a critical concentration.

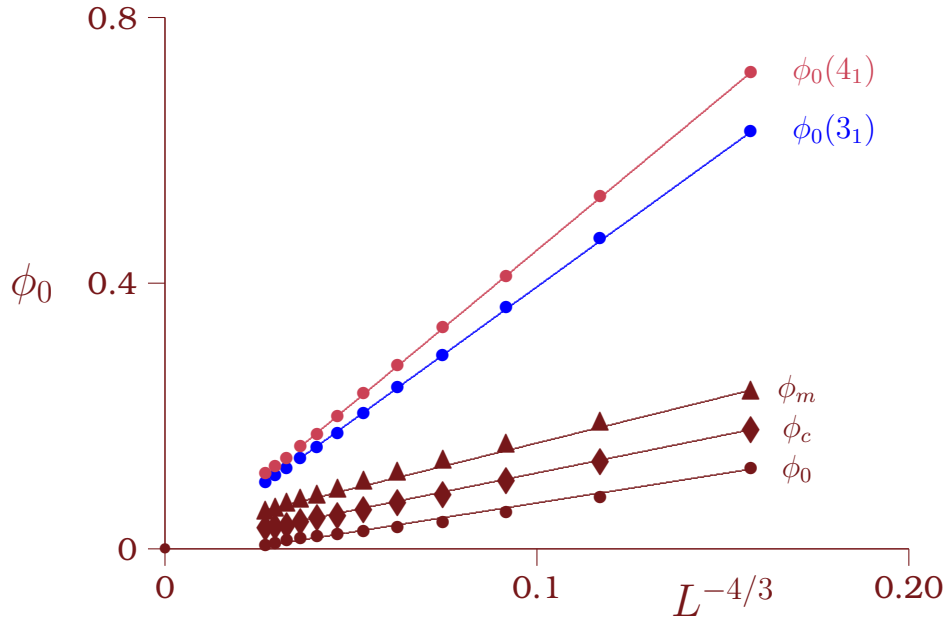


Figure 11: The critical concentration for the unknot (lowest three sets of data points denote by  $\bullet$  for  $\phi_0$ ,  $\blacklozenge$  for  $\phi_c$  and  $\blacktriangle$  for  $\phi_m$ ). The data for the concentration  $\phi_0$  for the trefoil knot are denoted by bullets (second set from above), and by  $\circ$  for the figure eight knot (top set of points).

For small values of the concentration the data in figure 9 is magnified in figure 10. This shows that there is an interval  $[\phi_0, \phi_m]$  so that the pressure is negative when  $\phi_0 < \phi < \phi_m$ . The pressure also goes through a minimum at a critical concentration  $\phi_c$ . The negative osmotic pressure corresponds to a regime when the lattice knot will tend to grow in length by adding edges. With increasing volume of the confining cube, these concentrations, namely  $\{\phi_0, \phi_c, \phi_m\}$ , approach zero.

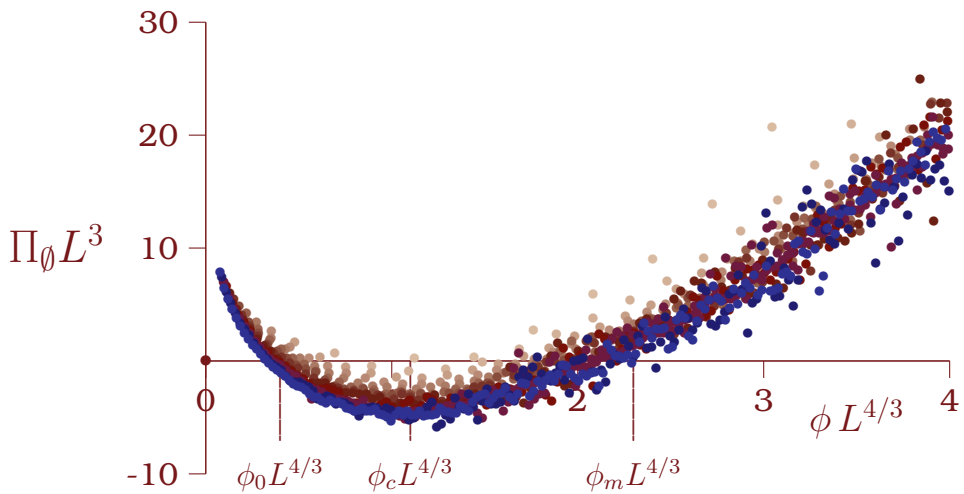


Figure 12: The rescaled osmotic pressure for unknotted compressed polygons plotted against the rescaled concentration. There is relative good data collapse, and this exposes the rescaled values of the critical values of the concentrations  $\phi_0 L^{4/3}$ ,  $\phi_m L^{4/3}$  and  $\phi_c L^{4/3}$ .

Since a lattice knot of length  $n$  will have linear size  $O(n^\nu)$ , it will start to fill the confining cube when  $n^\nu \sim L$ , or when  $n \sim L^{1/\nu}$ . This is the concentration where the osmotic pressure should vanish, and since  $\phi = \frac{n}{V}$ , the critical concentration  $\phi_m$  should be a function of  $L$ :

$$\phi_m \sim L^{1/\nu-3} \approx L^{-4/3}, \quad (21)$$

where the Flory value  $\nu = \frac{3}{5}$  was used. The same scaling should apply to  $\phi_0$  and  $\phi_c$ . In figure 11 the critical concentrations  $\{\phi_0, \phi_c, \phi_m\}$  are plotted against  $L^{-4/3}$ , and these data support a linear relationship. This shows, for example, that  $\phi_c \simeq 0.209 L^{-4/3}$ . Similarly,  $\phi_0 \simeq 0.149 L^{-4/3}$  and  $\phi_m \simeq 0.286 L^{-4/3}$ .

Equation (9) shows, that for  $\phi \rightarrow 0^+$ ,  $\Pi_\emptyset V = O(1)$ . In other words since  $\phi_c$  is small and decreasing to zero as  $L$  increases, one expects  $\Pi_\emptyset|_{\phi_c} \sim L^{-3}$ . If equation (22) is also taken into account, then rescaling the osmotic pressure and concentration by plotting  $\Pi_\emptyset L^3$  as a function of  $\phi L^{4/3}$  should collapse the data in figure 10 to a single underlying curve. This is seen by rescaling and replotted the data in figure 12. These data are still very noisy but for the larger values of  $L$  the data appear to cluster along a limiting curve.

### 3.2. Compressed lattice knots of knot types $3_1$ and $4_1$

**3.2.1. The free energy of compressed lattice knots of types  $3_1$  and  $4_1$ :** The free energy per unit volume  $F_V(K)$  of lattice knots of knot types  $3_1$  and  $4_1$  are plotted in figure 13 for lattice knots confined to cubes of dimension  $L$  and for  $L = 4, 5, \dots, 12$ . With increasing  $L$  the curves appear to approach a limiting curve which looks similar to the curves for  $F_V(\emptyset)$  in figure 5 (the free energy per unit volume for the unknot).

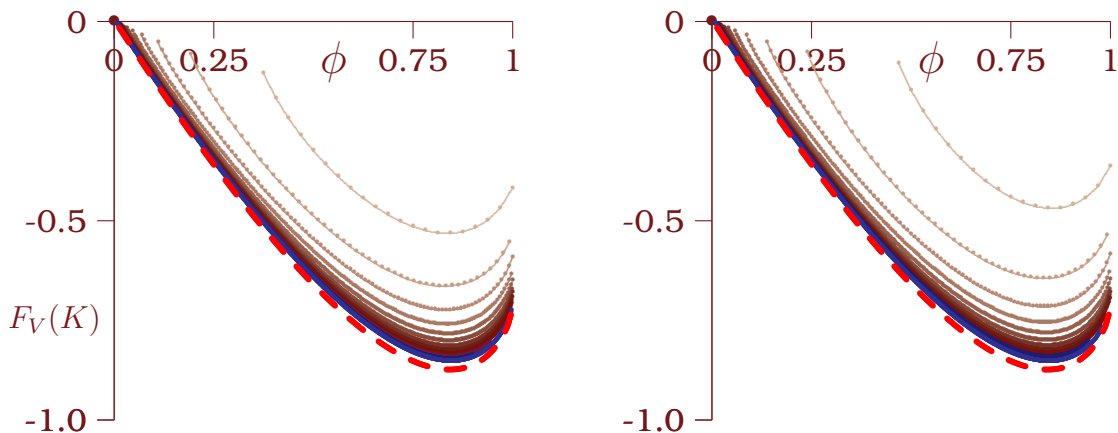


Figure 13: The free energies  $F_V(K)$  of compressed lattice knots confined to cubes of dimension  $L$ , with  $L \in \{3, 4, 5, \dots, 15\}$  and for knot types the trefoil (left panel) and the figure eight knot (right panel). With increasing values of  $L$  the curves systematically decrease to an apparent limiting free energy per unit volume given approximately by equation (22). In this particular graphs,  $\chi_K = 0.18$  and  $a_0 = 1 - \log \mu_3(\emptyset)$ ; see equation (18). Notice the differences between the left and right panels for smaller values of  $L$ .

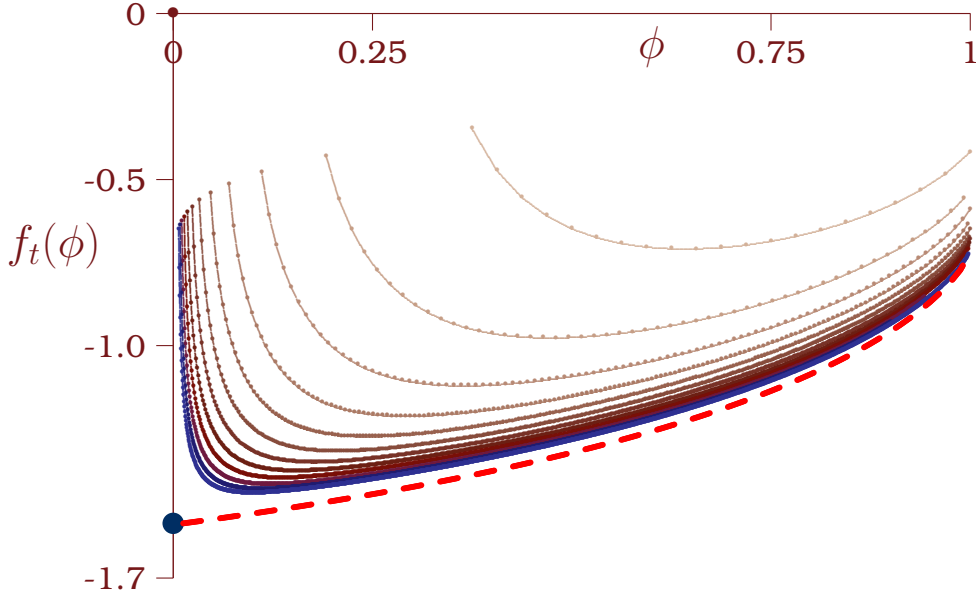


Figure 14: The free energy  $f_t(3_1)$  of compressed lattice knots of type the trefoil ( $3_1$ ) confined in cubes of dimension  $L$ , with  $L \in \{3, 4, 5, \dots, 15\}$ . With increasing values of  $L$  the curves systematically decrease to a hypothetical limiting curve. The dashed line is given by equation (16) with  $\chi_{01} = 0.18$  and  $a_0 = 1 - \log \mu_3(\emptyset)$ , showing that the values of the unknot gives a good approximation to the limiting curve.

Assuming the model in equation (8) gives the model

$$F_V(K) \simeq a_0\phi + (1 - \phi) \log(1 - \phi) - \chi_K \phi^2 \quad (22)$$

where  $\chi_K$  is the Flory interaction parameter for lattice knots of type  $K$ . Least squares fits of this model to the data in figure 13 give the estimates for  $\chi_{31}$  and  $\chi_{41}$  in the third and fourth columns of table 2. The estimates for  $\chi_{31}$  and  $\chi_{41}$  are significantly larger than for  $\chi_{01}$  for small values of  $L$  (say for  $L < 8$ ), but for  $L > 10$  the estimates converge to those measured for  $\chi_{01}$ . These estimates are plotted in figure 6, with  $\chi_{31}$  represented by  $\blacklozenge$ , and  $\chi_{41}$  by  $\blacksquare$ . Clearly, with increasing  $L$ , these estimates appear to converge to the same limiting values estimated for  $\chi_{01}$  (denoted by  $\bullet$ ).

The free energy per unit length,  $f_t(K)$ , is shown in figure 14 for lattice knots of knot type the trefoil, and in figure 15 for lattice knots of knot type the figure eight knot. The shapes of these curves are different from the results seen for the unknot in figure 7, and in particular at small values of the concentration and also for smaller values of  $L$ .

Minimal length lattice knots of knot type the unknot have little configurational entropy, but also has a relatively large contribution to its free energy arising translational degrees of freedom at low concentration.

On the other hand, minimal length lattice trefoil and figure eight knots have a substantial configurational entropy, in addition to contributions from translational degrees of freedom at low concentration. The configurational

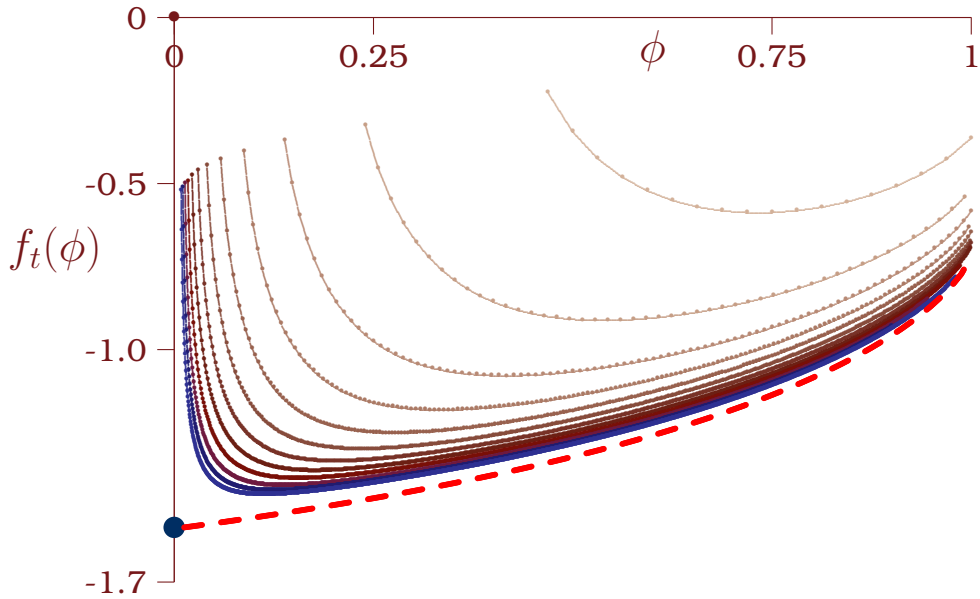


Figure 15: The free energy  $f_t(4_1)$  of compressed lattice knots of type the figure eight knot ( $4_1$ ) confined in cubes of dimension  $L$ , with  $L \in \{3, 4, 5, \dots, 15\}$ . With increasing values of  $L$  the curves systematically decrease to a hypothetical limiting curve. The dashed line is given by equation (16) with  $\chi_{01} = 0.18$  and  $a_0 = 1 - \log \mu_3(\emptyset)$ , showing that the values of the unknot gives a good approximation to the limiting curve.

entropy apparently underlies the differences seen between figures 7 for the unknot, and figures 14 and 15 for the trefoil and figure eight knots, respectively. These differences are illustrated in figure 16 for  $L = 10$ , and

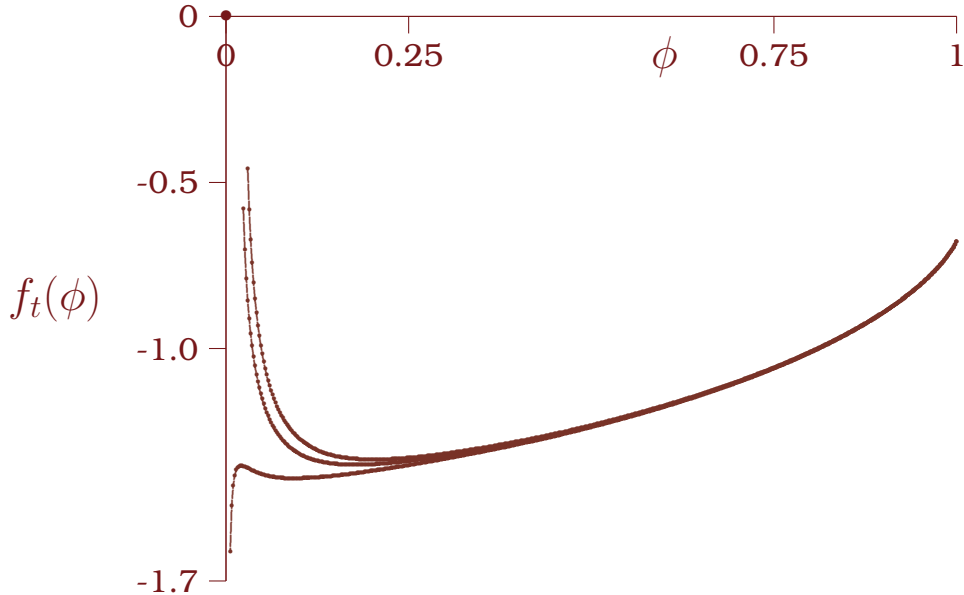


Figure 16: The free energies  $f_t(K)$  of compressed lattice knots with  $K = 0_1$  (bottom curve – the unknot),  $K = 3_1$  (middle curve – the trefoil) and  $K = 4_1$  (top curve – the figure eight knot). The lattice knots were confined in a cube of dimension  $L = 10$ .

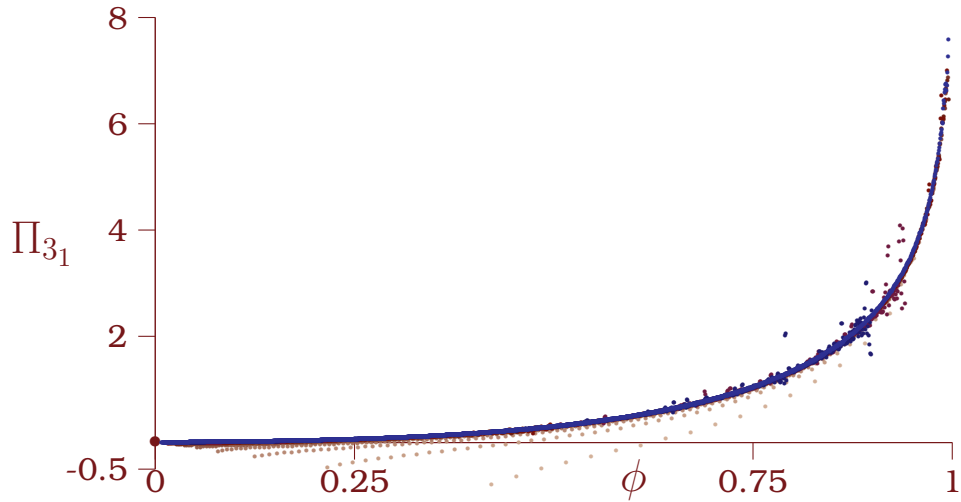


Figure 17: Osmotic pressure  $\Pi_{3_1}$  for compressed unknot lattice polygons determined by equation (19).

the free energies  $f_t(K)$  are plotted for the knot types the unknot, the trefoil and the figure eight knot. The differences are particularly prominent for low values of the concentration.

The analysis of the data for  $f_t(K)$  proceeded in the same way as for the unknot. The minimum free energy was determined by finding the concentration  $\phi^*$  at the minimum of the curves in figures 14 and 15, and fitting the Flory-Huggins model to data with concentrations  $\phi > \phi^*$ . This gives estimates for the Flory Interaction Parameter  $\chi_K$  for compressed knotted polygons. The results are in the second and third columns of table 3, and also plotted in figure 6 where the data points  $\diamond$  correspond to the results for the trefoil knot  $3_1$ , and the data points  $\square$  correspond to the results for the figure eight knot  $4_1$ . These results indicate that the estimate of the Flory interaction parameter  $\chi_K$  for knotted polygons is, in the limit that  $L \rightarrow \infty$ , the same as for the unknot and that equation (17) remains the best estimate in this study.

**3.2.2. The osmotic pressure of compressed lattice knots of types  $3_1$  and  $4_1$ :** The osmotic pressure of compressed lattice polygons of knot types  $3_1$  and  $4_1$  were computed using the numerical approximaton to the derivative in equation (19) and plotted in figures 17 and 18. At the scale of these figures there are little difference with the pressure seen for unknot lattice polygons in figure 9, but in view of figure 16 there must be differences at low values of the concentration  $\phi$ .

In the case of these non-trivial knot types, the osmotic pressure similarly turns negative at low concentration. However, the shapes of the low concentration osmotic pressure graphs differ from that of the unknot in figure 10, as shown in figures 19.

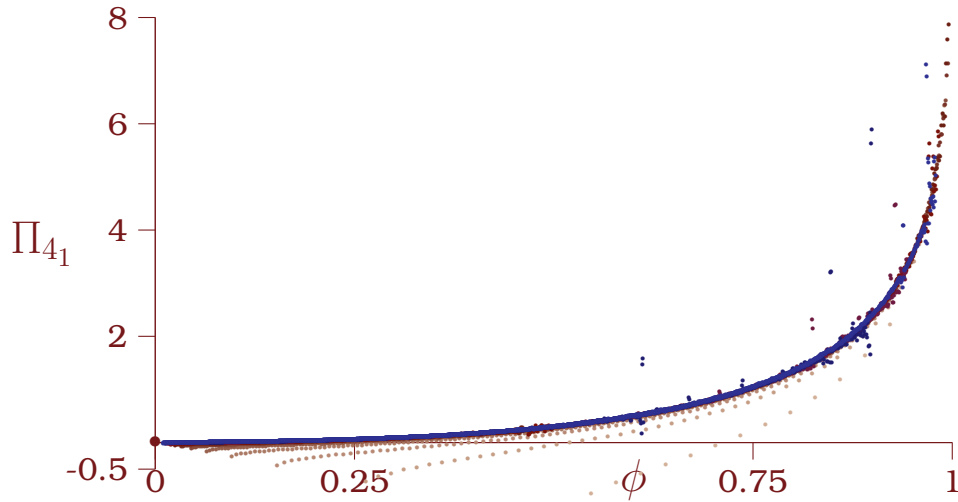


Figure 18: Osmotic pressure  $\Pi_{41}$  for compressed unknotted lattice polygons determined by equation (19).

At a critical value of the concentration,  $\phi_0$ , the osmotic pressure vanishes. The critical concentration  $\phi_0$  is a function of  $L$  and also a function of knot type, as shown by comparing the left and right panels in figure 19.

Negative osmotic pressures can be seen in figures 17 and 18, and the magnification of the axes in figure 19 confirms this. The data here show that these pressure curves are different from those observed for the unknot (see figure 9) since there are no local minima in these curves. Instead, the osmotic pressures for the knot types  $3_1$  and  $4_1$  increase monotonically from a negative value of low concentration, through a zero point at a critical concentration  $\phi_0$ , to positive osmotic pressures with increasing concentration when  $\phi > \phi_0$ .

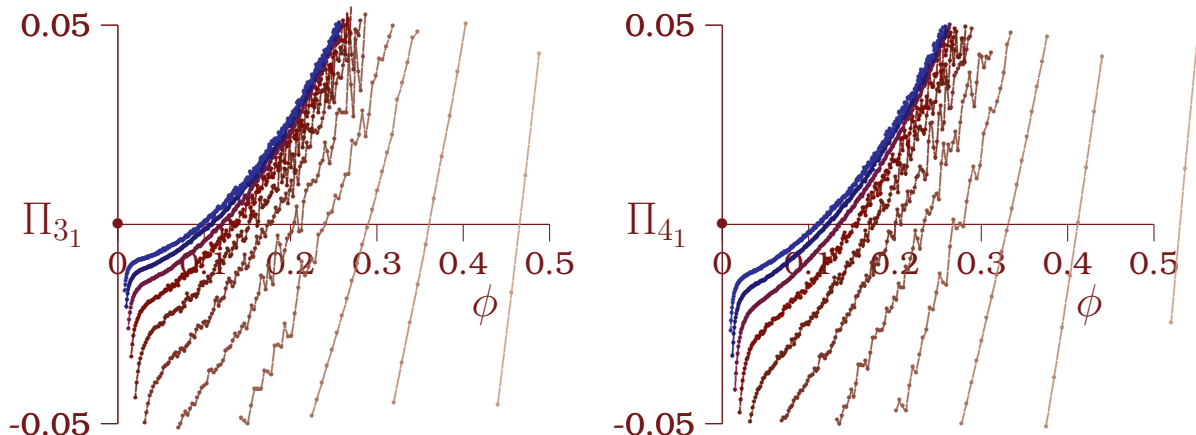


Figure 19: The osmotic pressures  $\Pi_{3_1}$  (left panel) and  $\Pi_{4_1}$  (right panel) for compressed lattice knots of knot types  $3_1$  and  $4_1$ . Both pressures are negative at low concentration, passing through critical concentration  $\phi_0$  where the pressure is zero, to positive osmotic pressure for higher concentration.

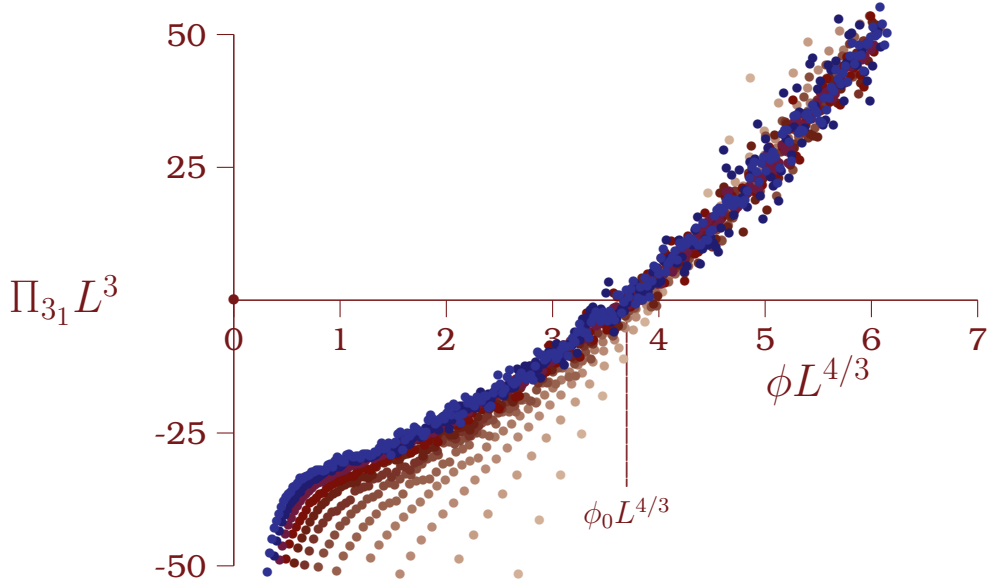


Figure 20: The rescaled osmotic pressure for compressed lattice knots of knot type  $3_1$  plotted against the rescaled concentration. There is relative good data collapse for concentrations  $\phi > \phi_0$ . If  $\phi < \phi_0$  the lattice knot has negative osmotic pressure, so that it will add length until the concentration approaches  $\phi_0$ . For  $\phi > \phi_0$  the osmotic pressure is positive, and the lattice knot will tend to shrink in length. These data show that  $\phi_0 L^{4/3} \approx 3.94$ .

If  $\phi < \phi_0$  the lattice knot has negative osmotic pressure, so that it will add length until the concentration approaches  $\phi_0$ . For  $\phi > \phi_0$  the osmotic pressure is positive, and the lattice knot will tend to shrink in length.

Since a lattice knot of length  $n$  will have linear size  $O(n^\nu)$ , it will start to fill the confining cube when  $n^\nu \sim L$ , or when  $n \sim L^{1/\nu}$ . This is the concentration where the osmotic pressure should vanish, and since  $\phi = \frac{n}{V}$ , the critical concentration  $\phi_0$  should be a function of  $L$ :

$$\phi_0 \sim L^{1/\nu-3} \approx L^{-4/3}, \quad (23)$$

where the Flory value  $\nu = \frac{3}{5}$  was used.

In figure 11 the critical concentration  $\phi_0$  for knot types  $3_1$  and  $4_1$  are plotted against  $L^{-4/3}$ , and the this graph supports this relationship. For the trefoil, a least squares fit gives  $\phi_0 \approx 3.94 L^{-4/3}$ , and for the figure eight knot,  $\phi_0 \approx 4.48 L^{-4/3}$ .

As before it follows from equation (9), that for  $\phi \rightarrow 0^+$ ,  $\Pi_K V = O(1)$ . Since  $\phi_0$  is small and decreasing to zero as  $L$  increases,  $\Pi_K|_{\phi_0} \sim L^{-3}$ . By equation (22) the osmotic pressure can be rescaled by plotting  $\Pi_K L^3$  as a function of  $\phi L^{4/3}$  and this should collapse the data in figure 19 to single underlying curves. This is seen by rescaling and replotting the data in figures 20 and 21. These plots are still very noisy by for concentrations  $\phi > \phi_0$  the data appear to cluster along limiting curves.

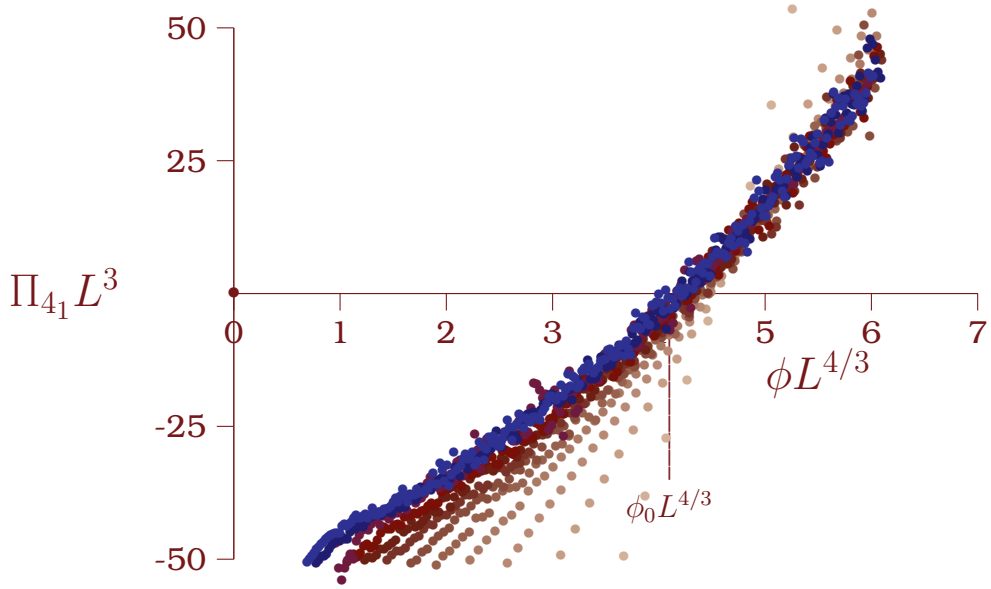


Figure 21: The rescaled osmotic pressure for compressed lattice knots of knot type  $4_1$  plotted against the rescaled concentration. There is relative good data collapse for concentrations  $\phi > \phi_0$ . If  $\phi < \phi_0$  the lattice knot has negative osmotic pressure, so that it will add length until the concentration approaches  $\phi_0$ . For  $\phi > \phi_0$  the osmotic pressure is positive, and the lattice knot will tend to shrink in length. These data show that  $\phi_0 L^{4/3} \approx 4.48$ .

#### 4. Conclusions

The mean field expressions for the free energies in Flory-Huggins theory are good approximations to the free energy of a model of compressed lattice polygons in a cube of dimension  $L$ . This is, for example, seen in the data plotted in figure 5 and in figure 7. It was also possible to determine a consistent value of the Flory Interaction Parameter  $\chi$  from the data, as shown in figure 6.

There are, however, some additional observations which can be made about using Flory-Huggins theory to model the free energy of compressed lattice knots. These are

- The results support the notion that the Flory Interaction Parameter is independent of knot type;
- While the Flory-Huggins expressions in equation (14) and equation (16) are good approximations of the free energies  $F_V$  and  $f_t$ , the Flory Huggins expression for the osmotic pressure in equation (9) deviates from the calculated data in figures 9, 17 and 18, in particular at higher concentration;
- On magnification of the osmotic pressure in figures 10 and 19, Flory-Huggins theory is not a good approximation at low concentrations – it fails to explain the dependence of osmotic pressure on knot type, and

does not account for the negative values of the osmotic pressure in the data.

Instead, directly determining the osmotic pressure from our data gives the results in figures 9, 17 and 18. Examination and rescaling of the data in these figures at low concentration give figures 12, 20 and 21. This shows that the osmotic pressure is dependent on knot type, and that this dependence can be quantified by calculating the critical concentrations  $\{\phi_0, \phi_c, \phi_m\}$  for the unknot, and  $\phi_0$  for the trefoil and figure eight knot.

**Acknowledgements:** EJJvR acknowledges financial support from NSERC (Canada) in the form of a Discovery Grant. We are grateful to SG Whittington for helpful remarks and advice.

## References

- [1] C Aragao de Carvalho, S Caracciolo, and J Fröhlich. Polymers and  $g\phi^4$ -theory in four dimensions. *Nucl Phys B*, 215:209–248, 1983.
- [2] M Baiesi, E Orlandini, and AL Stella. The entropic cost to tie a knot. *J Stat Mech: Theo Expr*, page P06012, 2010.
- [3] B Berg and D Foerster. Random paths and random surfaces on a digital computer. *Phys Lett B*, 106:323–326, 1981.
- [4] I Carmesin and K Kremer. The bond fluctuation method: A new effective algorithm for the dynamics of polymers in all spatial dimensions. *Macromol*, 21(9):2819–2823, 1988.
- [5] NR Cozzarelli and JC Wang. *DNA topology and its biological effects*. Cold Spring Harbor Laboratory Press, 1990.
- [6] P-G de Gennes. Collapse of a polymer chain in poor solvents. *J de Phys Lett*, 36:55–57, 1975.
- [7] P-G de Gennes. *Scaling Concepts in Polymer Physics*. Cornell, 1979.
- [8] P-G de Gennes. Tight knots. *Macromol*, 17:703–704, 1984.
- [9] M Delbrück. Knotting problems in biology. *Proc Symp Appl Math*, 14:55–63, 1962.
- [10] SF Edwards. Statistical mechanics with topological constraints: I. *Proc Phys Soc*, 91(3):513, 1967.
- [11] SF Edwards. In *Molecular fluids: Les Houches, Aout 1973, Cours de l'Ecole de Physique Theorique*, Eds. R Balian and G Weill. Gordon & Breach, New York, 1976.
- [12] PJ Flory. Thermodynamics of high polymer solutions. *J Chem Phys*, 10:51–61, 1942.
- [13] PJ Flory. *Principles of Polymer Chemistry*. Cornell University Press, London, 1953.
- [14] F Gassoumov and EJ Janse van Rensburg. Osmotic pressure of confined square lattice self-avoiding walks. *arXiv : cond-mat*, 1806.01746, 2018.
- [15] ML Huggins. Some properties of solutions of long-chain compounds. *J Phys Chem*, 46:151–158, 1942.
- [16] EJ Janse van Rensburg and A Rechnitzer. Generalized atmospheric sampling of self-avoiding walks. *J Phys A: Math Theo*, 42:335001, 2009.
- [17] EJ Janse van Rensburg and A Rechnitzer. Generalized atmospheric sampling of knotted polygons. *J Knot Theo Ram*, 20:1145–1171, 2011.
- [18] EJ Janse van Rensburg and SG Whittington. The knot probability in lattice polygons. *J Phys A: Math Gen*, 23:3574–3590, 1990.

- [19] EJ Janse van Rensburg and SG Whittington. The BFACF algorithm and knotted polygons. *J Phys A: Math Gen*, 24:5553–5567, 1991.
- [20] D Jungreis. Gaussian random polygons are globally knotted. *J Knot Theo Ram*, 3:455–464, 1994.
- [21] K Koniaris and M Muthukumar. Knottedness in ring polymers. *Phys Rev Lett*, 66:2211–2214, 1991.
- [22] Y Liu and B Chakraborty. Shapes of semiflexible polymers in confined spaces. *Phys Biol*, 5(2):026004, 2008.
- [23] Y Liu and B Chakraborty. Segregation of polymers in confined spaces. *Phys Biol*, 9(6):066005, 2012.
- [24] B Marcone, E Orlandini, AL Stella, and F Zonta. What is the length of a knot in a polymer? *J Phys A: Math Gen*, 38:L15–L21, 2004.
- [25] R Matthews, AA Louis, and JM Yeomans. Confinement of knotted polymers in a slit. *Mol Phys*, 109:1289–1295, 2011.
- [26] C Micheletti, D Marenduzzo, E Orlandini, and DW Summers. Knotting of random ring polymers in confined spaces. *J Chem Phys*, 124(6):064903, 2006.
- [27] C Micheletti and E Orlandini. Numerical study of linear and circular model DNA chains confined in a slit: metric and topological properties. *Macromol*, 45(4):2113–2121, 2012.
- [28] JPJ Michels and FW Wiegel. Probability of knots in a polymer ring. *Phys Lett A*, 90:381–384, 1982.
- [29] M Müller, JP Wittmer, and ME Cates. Topological effects in ring polymers: A computer simulation study. *Phys Rev E*, 53(5):5063–5074, 1996.
- [30] E Orlandini, AL Stella, and C Vanderzande. The size of knots in polymers. *Phys Biol*, 6(2):025012, 2009.
- [31] E Orlandini, MC Tesi, EJ Janse van Rensburg, and SG Whittington. Entropic exponents of lattice polygons with specified knot type. *J Phys A: Math Gen*, 29:L299–L304, 1996.
- [32] E Orlandini and SG Whittington. Statistical topology of closed curves: Some applications in polymer physics. *Rev Mod Phys*, 79(2):611, 2007.
- [33] N Pippenger. Knots in random walks. *Disc Appl Math*, 25:273–278, 1989.
- [34] VV Rybenkov, NR Cozzarelli, and AV Vologodskii. Probability of DNA knotting and the effective diameter of the DNA double helix. *Proc Nat Acad Sci*, 90:5307–5311, 1993.
- [35] VV Rybenkov, AV Vologodskii, and NR Cozzarelli. The effect of ionic conditions on DNA helical repeat, effective diameter and free energy of supercoiling. *Nucl Acids Res*, 25:1412–1418, 1997.
- [36] R Scharein, K Ishihara, J Arsuaga, Y Diao, K Shimokawa, and M Vazquez. Bounds for the minimum step number of knots in the simple cubic lattice. *J Phys A: Math Theo*, 42:475006, 2009.
- [37] SY Shaw and JC Wang. Knotting of a DNA chain during ring closure. *Science*, 260:533–536, 1993.
- [38] CE Soteros. Random knots in uniform branched polymers. *Math Modelling Sci Comp*, 2:747–752, 1993.
- [39] CE Soteros. Knots in graphs in subsets of  $\mathbb{N}^3$ . In SG Whittington, DW Sumners and T Lodge, editor, *Topology and Geometry in Polymer Science*, pages 101–133. Springer, 1998.
- [40] JM Stephen. Collapse of a polymer chain. *Phys Lett A*, 53:363–364, 1975.
- [41] DW Sumners and SG Whittington. Knots in self-avoiding walks. *J Phys A: Math Gen*, 21:1689–1694, 1988.
- [42] MC Tesi, EJ Janse van Rensburg, E Orlandini, DW Sumners, and SG Whittington. Knotting and supercoiling in circular DNA: A model incorporating the effect of added salt. *Phys Rev E*, 49:868–872, 1994.

- [43] S Trigueros, J Arsuaga, ME Vazquez, DW Sumners, and J Roca. Novel display of knotted DNA molecules by two-dimensional gel electrophoresis. *Nucl Acids Res*, 29:e67–e67, 2001.
- [44] AV Vologodskii, AV Lukashin, MD Frank-Kamenetskii, and VV Anshelevich. The knot problem in statistical mechanics of polymer chains. *Sov J Expr Theo Phys*, 39:1059–1063, 1974.
- [45] SG Whittington and EJ Janse van Rensburg. Random knots in ring polymers. *Math Mod and Sci Comp*, 2:741–746, 1993.